Ultra-sensitive LC MEMS for bladder pressure monitoring using modified slotted diaphragm

L. Tahar [*], K. Malika
*Laboratory of Electronic Photonic and Optronic (LEPO), Department of
Electronic, Djillali Liabes University, Sidi Bel Abbes 22000, Algeria*

In this paper, we have designed and simulated an implantable MEMS-based LC pressure sensor for bladder pressure monitoring. The device is composed of metal-insulator-metal capacitive sensor in which the size of the diaphragm is 1 mm × 1 mm of 5 μm thickness. Besides, novel modified-slotted diaphragm is developed to improve the sensitivity by decreasing the mechanical rigidity of the membrane. We used the COMSOL Multiphysics a tool for design and simulation. According to the results, the frequency response to the variable pressure is varied within the range of 35.23 to 119.72 MHz, the results also yield a value obtained of the quality factor is worth 32 with high value of 4.22 kHz/Pa sensor sensitivity. Hence, this sensor with a novel modified-slotted diaphragm has a high-pressure sensitivity, which shows 2.91 times more sensitivity than clamped diaphragm.

1. Introduction

Benign prostatic hyperplasia (BPH) is a histologic change, in which the stromal cells in the transition zone of the prostate gland develop out of control. Some diseases are associated with BPH like Bladder dysfunction, Lower urinary tract symptoms (LUTS), and stress urinary incontinence (UI) [1]; [2] prove that the pandemic of coronavirus diseases 2019 (COVID-19) can responsible for the development of BPH. Men with BPH have an increased risk of prostate cancer, according to epidemiological research [3]. In 2018, bladder cancer was the sixth most frequent cancer in men [4]. The patient's bladder pressure rises as a result of the residual urine. As a result, monitoring bladder pressure is a simple way to diagnose early BPH. Urodynamic testing is a non-invasive method of checking the bladder's function. However, exactly reproducing the patient's real voiding pattern may be difficult [5]. A cystometry examination was now used, but this procedure is non-physiological and caused patients severe discomfort [6]. Implantable devices have been investigated to achieve precise bladder pressure monitoring [7]. The pressure in the bladder ranges from 0 to 20 kPa [8]. Putting an implantable pressure sensor into the urine bladder can help people feel better.

Microelectromechanical systems (MEMS) technology can be used to monitor bladder pressure. Passive telemetry of inductor-capacitor (LC) based on MEMS is preferred in implanted sensors because this passive wireless sensor does not need a battery to work [6]. Capacitive pressure sensors were chosen for this study because of their low power consumption, great temperature insensitivity, low cost, and high sensitivity [9]. In terms of size, Implants sensors should have a surface area of fewer than 1 cm^2. [5]. [10] propose an implantable LC sensor with 6 mm^2.

In the development of implantable MEMS materials, Silicon and metallic ox-ides were proposed. However, these materials have imposed damage to soft tissues [11]. Then, Silicone elastomer has been used as a substrate, while offering conformal encapsulation of the implantable sensors [12]. PDMS has the characteristic of biocompatibility and ease of processing [13].

According to [14], doping silicone oil can dramatically reduce the mechanical properties of PDMS.

Several structures, such as circular and square membranes have been created [15, 16]. Various researchers in the past have changed the clamped simple diaphragm to create slotted, corrugated, or bossed [17]. Making slots around the membrane can actually lower diaphragm flexibility. It increases the mechanical sensitivity of the diaphragm by causing increased membrane deflection. [18] presents an innovative C-slotted structure. In the instance of bladder pressure sensing, [19] found that a slotted diaphragm had superior sensitivity to a clamped diaphragm.

The primary objective of this study is to overcome the disadvantages of previous studies by developing a novel LC MEMS pressure sensor with a modified-slotted diaphragm, resulting in a small size, high safe frequency response, and improved sensor sensitivity by reducing the mechanical stiffness of the encapsulation. Those characteristics give the sensor the possibility to be implanted in intravesical.

2. Materials and methods

Figure 1 shows the schematic diagram of the LC sensing system for the bladder pressure monitoring system. We have designed and simulated an implantable MEMS-based LC pressure sensor for bladder pressure monitoring. The device is composed of metal-insulator-metal capacitive sensor in which the size of the diaphragm is 1 mm × 1 mm of 5 µm thickness. The LC pressure sensor was modeled using a variable MEMS capacitor, C_s; a series resistance, R_s=58.4 Ω, and a micro-inductor, L_s=2.49 µH [20]. The external coil is represented by the inductance, L_e, which is connected to the resistance, R_e.
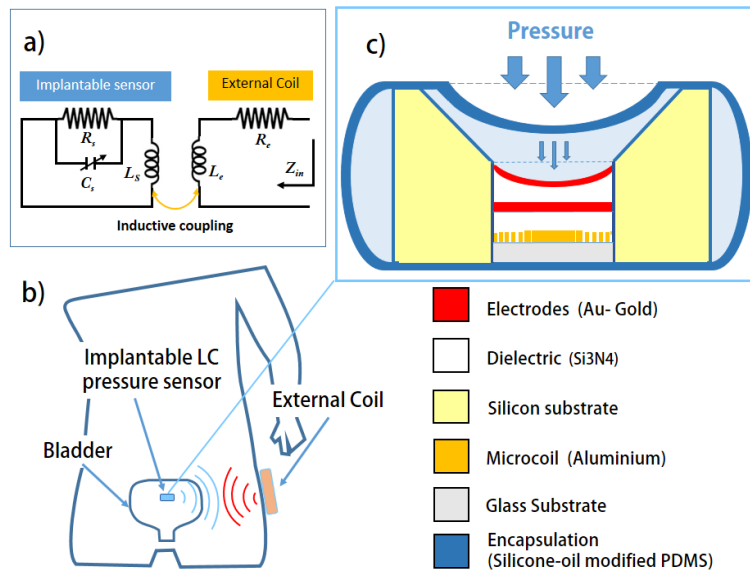
Fig. 1. Schematic diagram of the LC sensing system. (a) LC wireless sensing system's electrical model; (b) LC sensing system within the human bladder; (c) Cross-section of implantable sensitive capsule after contact pressure.

The deflection in the diaphragm causes tension in the MEMS capacitive pressure sensor by moving the flexible membrane towards the fixed plate, which aids in measuring the displacement by pressure change [20]. The capacitance, C_s, is expressed as [16]

$$C_s = \varepsilon_0 \varepsilon_r \frac{A}{d} \tag{1}$$

where ε_r is the relative permittivity of the medium in between the plates, ε_0 is the permittivity, A is the surface of the plate and d is the thickness of the insulating layer. The equations relate to the sensor's resonant frequency, f can be retrieved as follows [21]

$$f = \frac{1}{2\pi\sqrt{LC}}$$ (2)

As for the value of the quality factor, Q, it can be expressed as

$$Q = \frac{\omega_0 L}{R}$$ (3)

where ω_0 is the angular resonance frequency ($\omega_0 = 2\pi f$), R is the coil resistance value and L is the value of micro-inductance. The geometry of the diaphragm is unique for this structure. A novel design can be obtained for a slotted diaphragm as shown in Fig. 2 and 3.
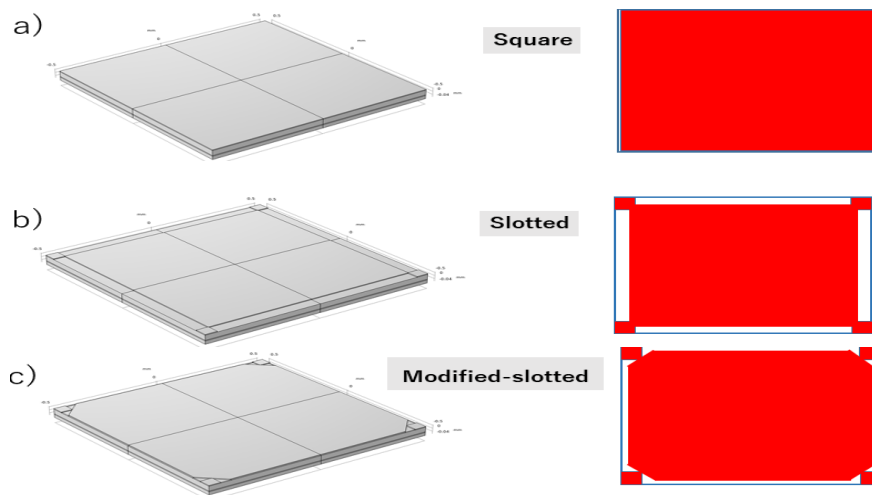
Fig. 2. Schematic view of the movable diaphragm. (a). clamped diaphragm. (b) Slotted diaphragm. (c) modified-slotted diaphragm.
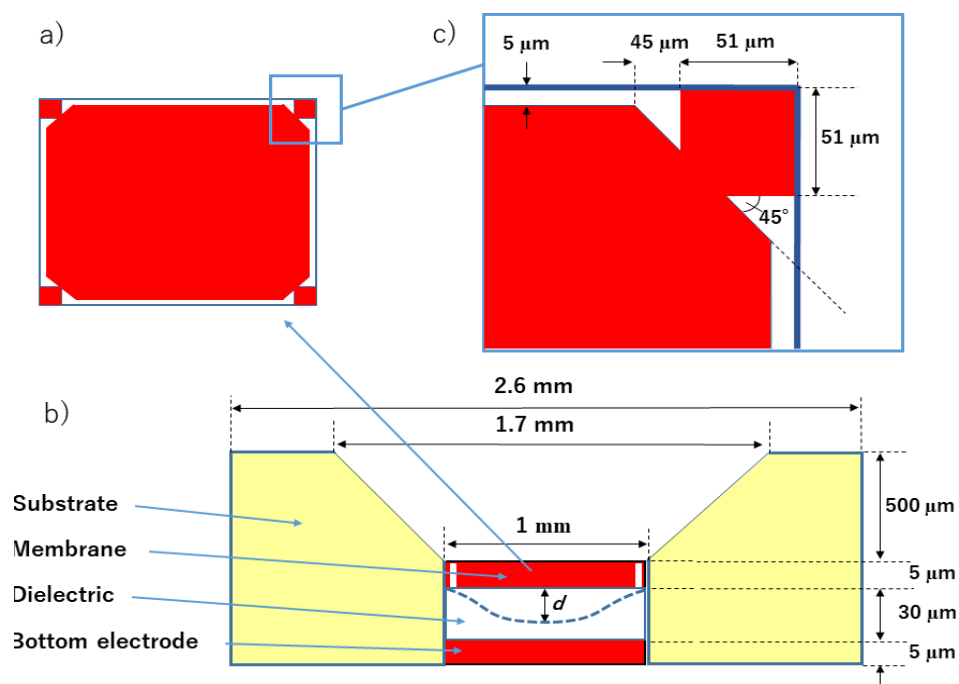
Fig. 3. Geometry details of proposed structure. (a) Top view of modified-slotted diaphragm. (b) Cross section of the capacitive MEMS. (c) Dimensions of the modified-slotted structure.

Making slots around the membrane can lower diaphragm flexibility. It increases the mechanical sensitivity of the diaphragm by causing increased membrane deflection. The material for the bottom electrode (gold) is the same as that of the diaphragm and its dimensions are 1 mm x 1 mm of 5 μm thickness. The thickness of the air gap is 30 μm. The total surface of the implantable sensor is 2.6 mm^2 with a thickness of 600 μm. To achieve ultra-sensitive implant sensors. The flexibility of the capsule must be very large using a soft implantable bioelectronics material. Silicon-oil modified PDMS is used for such purpose, it has a young's modulus of 0.567 MPa [14].

3. Finite element method

Using COMSOL Multiphysics 5.6, the performance of the LC sensor is analyzed and calculated using the Finite Element Method (FEM). Numerical simulation is not only suitable but also necessary from time to time when the experimental findings of operation are not visible. Fixed boundary conditions are used, and the proposed membrane is exposed to a pressure of 20 kPa. For the electrodes, The Au gold's characteristics are as follows: The Poisson ratio is 0.44, and Young's modulus is 70 MPa. For the dielectric, the relative permittivity of the proposed materials is as follows: silicon nitride (ε_r=9.7), zinc oxide (ε_r=8.3), aluminum oxide (ε_r=5.7), silicon dioxide (ε_r=4.2) and poly(methyl methacrylate) (ε_r=3). We fix one corner with regard to x-, y-, and z-displacements and rotation to obtain the boundary conditions for the Solid, Pressure interface. Additional details are on the model library path MEMS_Module/Sensors/capacitive_pressure_sensor.

4. Results and discussions

Using the FEM, Fig. 4 depicts the von Mises stress distribution for the diaphragm at a maximum pressure of 20 kPa. We observe that the stress is concentrated at the clamped membrane's borders. Nevertheless, in the modified-slotted membrane, the stress value in the center and borders is quite low.

Figure. 5 depicts the surface displacement for the diaphragm in maximum pressure 20 kPa using the FEM. We observe that the highest central deflection of a clamped diaphragm is 8.38 μm, while the maximum deflection of a modified-slotted diaphragm is 30.25 μm, which shows three times more than the clamped one.
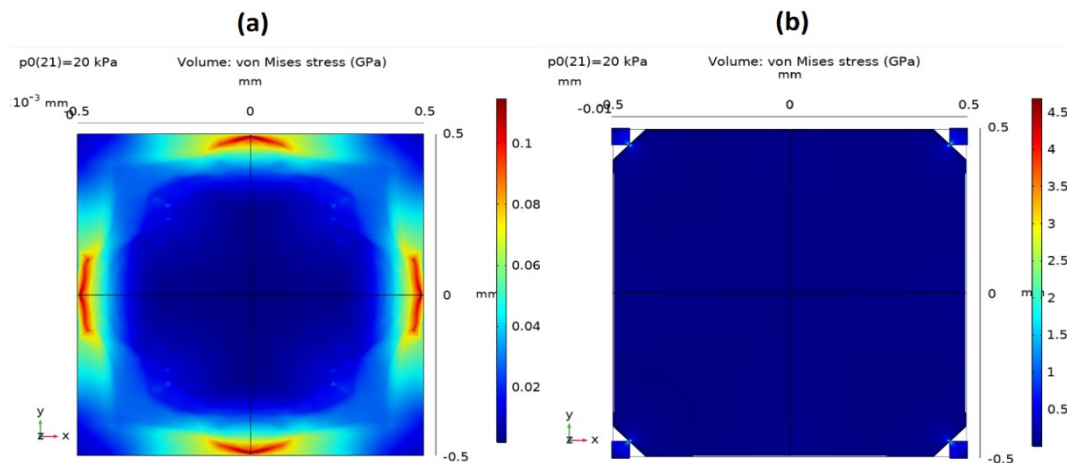
Fig. 4. Surface displacement on the (a) clamped diaphragm, (b) modified-slotted diaphragm.
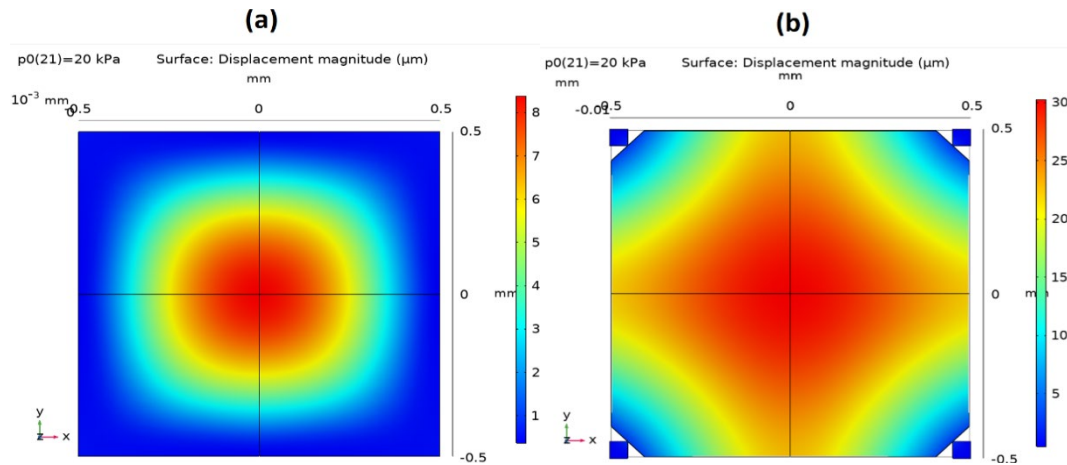
Fig. 5. Von Mises Stress distribution on the (a) clamped structure, (b) modified-slotted structure.

To get the maximum capacitance in pF, we simulate five different dielectric materials as shown in Fig. 6. Capacitive response of silicon nitride and zinc oxide dielectric are having the capacitance of 8.19 and 6.93 pF respectively. poly(methyl methacrylate) shows a low capacitance of 2.42 pF whereas aluminum oxide and silicon dioxide dielectric show capacitance of 4.68 and 3.41 pF, respectively. The maximum capacitance of conventional silicon nitride is compared with poly(methyl methacrylate) dielectric, which shows 3.38 times more capacitance than poly(methyl methacrylate). Figure 7 shows the capacitive responses of the MEMS pressure sensor from 0 to 20 kPa. We observe that the highest capacitive response of a clamped diaphragm is 0.79 pF and of a slotted diaphragm is 6.78 pF while the maximum deflection of a modified-slotted diaphragm is 8.19 pF, which shows 10.33 times more capacitive than the clamped one. As we show in part II, the sensor guarantees monitoring even at high bladder pressures, up to 20 kPa, which is higher than the pressures produced by rapid abdominal contractions, sports activities, or coughs.
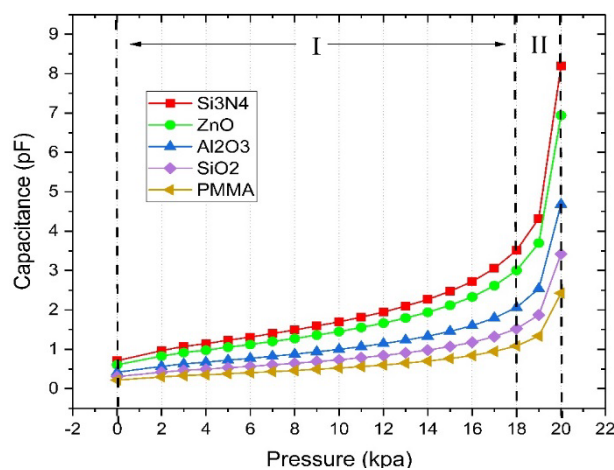
Fig. 6. Capacitance characteristics of modified-slotted diaphragm with different dielectric materials.
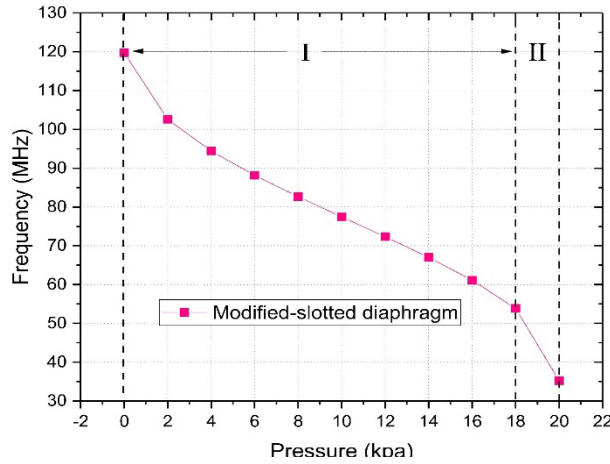
Fig. 7. Capacitive response of MEMS pressure sensor.
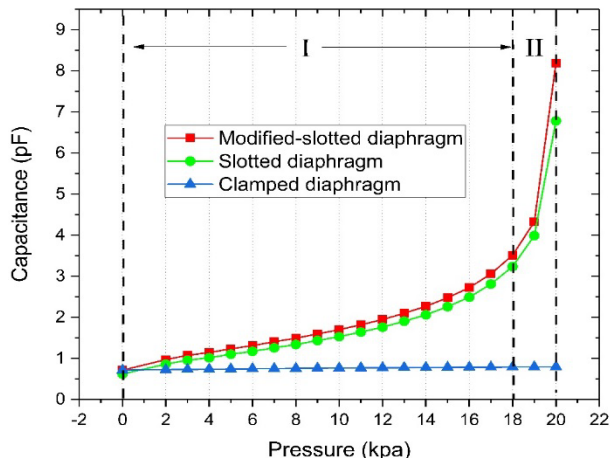
Fig. 8. Frequency response of proposed LC pressure sensor.

Figure 8 depicts the frequency response of the LC pressure sensor. The average value of the capacitive response from the modified-slotted diaphragm of the MEMS sensor recorded in Fig. 7 was used to calculate the value of this frequency using equation (2). The frequency response to the variable pressure is varied within the range of 35.23 to 119.72 MHz, as shown in Fig. 8. After applying equation (3), the value obtained of the quality factor for the operating frequency of 119.72 MHz is worth Q=32 with a high value of 4.22 kHz/Pa sensor sensitivity. This sensor with a novel modified-slotted diaphragm has a high-pressure sensitivity, which shows 2.91 times more sensitivity than [14] with the clamped diaphragm.

5. Conclusions

A novel LC MEMS pressure sensor for bladder pressure application is designed and simulated using the Finite Element Method (FEM). The size of the diaphragm is 1 mm × 1 mm of 5 μm thickness. Bladder pressure in humans typically ranges be-tween 0 and 20 kPa. According to the results, the frequency response to the variable pressure is varied within the range of 35.23 to 119.72 MHz, the results also yield a quality factor is worth 32 with a high value of 4.22 kHz/Pa sensor sensitivity. This sensor with a novel modified-slotted diaphragm has a high-pressure sensitivity, which shows 2.91 times more sensitivity than the clamped diaphragm. It is observed that the model Au/Si3N4/Au with a modified-slotted structure has good deflection, a high

capacitance response and it also yields good frequency sensitivity, hence this new structure has a better figure of merit rather than another LC-MEMS condenser diaphragm. Those characteristics give the sensor the possibility to be implanted in intravesical.

Acknowledgments

References

[1] P. Abrams, Reviews in Urology 1(2), 65(1999).
[2] A. Haghpanah, F. Masjedi, M. Salehipour, A. Hosseinpour, J. Roozbeh, A. Dehghani, Prostate Cancer and Prostatic Diseases 25, 27(2022); https://doi.org/10.1038/s41391-021-00388-3
[3] D. D. Ørsted, S. E. Bojesen, Nature Reviews Urology 10, 49(2013); https://doi.org/10.1038/nrurol.2012.192
[4] T. Kloskowski, K. Szeliski, K. Krzeszowiak, Z. Fekner, Ł. Kazimierski, A. Jundziłł, T. Drewa, M. Pokrywczyńska, Scientific Reports 11, 1(2021); https://doi.org/10.1038/s41598-021-01996-8
[5] H. Y. Lee, B. Choi, S. Kim, S. J. Kim, W. J. Bae and S. W. Kim, IEEE Sensor Journal 16(24), 4715 (2016).
[6] I. Clausen, L. G. W. Tvedt, T. Glott, Sensors 18(7), 2128(2018); https://doi.org/10.3390/s18072128
[7] S. J. Majerus, P. C. Fletter, M. S. Damaser, S. L. Garverick, IEEE Transactions on Biomedical Engineering 58, 763(2010).
[8] Q.-A. Huang, L. Dong and L.-F. Wang, Journal of Microelectromechanical Systems 25(5), 822 (2016).
[9] K. B. Balavalad, B. Sheeparamatti, Sensors & Transducers 187, 120(2015).
[10] N. Yusof, B. Bais, B. Y. Majlis, N. Soin, 2017 IEEE Regional Symposium on Micro and Nanoelectronics, 22(2017); https://doi.org/10.1109/RSM.2017.8069147
[11] L. Yu, B. J. Kim, E. Meng, Sensors 14(11), 20620(2014) https://doi.org/10.3390/s141120620
[12] Y. Chen, Y.-S. Kim, B. W. Tillman, W.-H. Yeo, Y. Chun, Materials 11(4), 522(2018); https://doi.org/10.3390/ma11040522
[13] S. Sang, H. Witte, Microsystem Technologies 16, 1001(2010) https://doi.org/10.1007/s00542-010-1077-x
[14] Y.-J. Lin, K.-H. Lin, Y.-S. Juan, C.-H. Lin, 2021 21st International Conference on Solid-State Sensors, Actuators and Microsystems (Transducers), 1142(2021).
[15] M. Mahdi, Microsystem Technologies 27, 2913(2021); https://doi.org/10.1007/s00542-020-05079-y
[16] K. Srinivasa Rao, V. Bala Teja, G. Krishnateja, P. Ashok Kumar, K. Ramesh, Microsystem Technologies 26, 1875(2020); https://doi.org/10.1007/s00542-019-04735-2
[17] B. A. Ganji, B. Y. Majlis, Microsystem Technologies 15, 1401(2009); https://doi.org/10.1007/s00542-009-0902-6
[18] B. Azizollah Ganji, S. Babaei Sedaghat, A. Roncaglia, L. Belsito, Microsystem Technologies 24, 3133(2018); https://doi.org/10.1007/s00542-018-3816-3
[19] G. Fragiacomo, K. Reck, L. Lorenzen, E. V. Thomsen, Sensors 10, 9541(2010); https://doi.org/10.3390/s101109541
[20] K. S. Rao, W. Samyuktha, D. V. Vardhan, B. G. Naidu, P. A. Kumar, K. G. Sravani, K. Guha, Microsystem Technologies 26, 2371(2020); https://doi.org/10.1007/s00542-020-04777-x
[21] N. Yusof, B. Bais, J. Yunas, N. Soin, B. Y. Majlis, Membranes 11(12), 996(2021) ; https://doi.org/10.3390/membranes11120996